Segmented Three-dimensional Echo-Planar Flow Imaging of the Cervical Carotid Arteries

Jean A. Tkach, Xiaoping Ding, Paul M. Ruggieri, Nancy A. Obuchowski, Michael Lieber, and Thomas J. Masaryk

PURPOSE: To implement and assess the application of segmented three-dimensional echo-planar MR imaging time-of-flight flow sequences for studying the anatomy of the cervical carotid arteries at 1.5 T. **METHODS:** The 3-D echo-planar sequences were segmented along the in-plane phase-encoding direction. Echo train lengths (ETLs) of 3 and 5 and signal bandwidths of ±25, ±33, and ±50 KHz were tested along with a conventional (ETL = 1) 3-D MR flow study in six healthy volunteers and in five patients with known arteriosclerotic disease involving the carotid bifurcation as confirmed by conventional angiography. The volunteer data were used to rank the techniques with respect to vessel dimension, vessel/background contrast, and quality by four trained neuroradiologists. For the patient studies, the percentage of stenoses was measured for all MR studies and compared against the conventional angiographic data using the criteria of the North American Symptomatic Carotid Endarterectomy Trial. **RESULTS:** Using Wilcoxon's test statistic and a significance level of .05, we found that the conventional MR flow examination was better than the segmented techniques and that the segmented techniques with ETL of 3 were superior to their counterparts with ETL of 5. For the ETL of 3 techniques, the high-bandwidth studies were inferior to their lower bandwidth counterparts; however, there was no significant difference between the performance of the medium- and low-bandwidth sequences. The patient data revealed that the segmented techniques consistently overestimated the severity of stenosis; however, in no instance did any of the segmented examinations erroneously indicate the presence of disease. **CONCLUSIONS:** The reduction in acquisition time and the zero false-positive rate we obtained suggest that segmented 3-D echo-planar MR flow techniques may be used as a screening/locating study for cervical carotid artery disease.

Index terms: Arteries, carotid; Magnetic resonance angiography

AJNR Am J Neuroradiol 18:1339–1347, August 1997

Segmented magnetic resonance (MR) acquisition schemes have found application in multiple areas of clinical MR imaging. The major benefit of these techniques is the reduction of examination time with minimal change in spatial resolution and/or image contrast. Multiple strategies, including echo-planar imaging and spiral k-space coverage, have been applied to MR angiography to reduce imaging time (1)(X. Ding, J. Tkach, T. J. Masaryk, "Fast 3-D Spiral Scan and Its Application in MRA," in: *Proceedings of the 3rd SMR/12th ESMRMB Joint Meeting,* 1995:422; and V. A. Magnotta, J. C. Ehrardt, X. Hong, et al, "Twenty-three Second 3-D Echo-Planer Time-of-Flight MRA of the Carotid Bifurcation," in: *Proceedings of the 3rd SMR/12th ESMRMB Joint Meeting,* 1995:570). However, both techniques are extremely sensitive to local static field inhomogeneities such that image quality is compromised (2, 3). These techniques are also more demanding in terms of imaging hardware and reconstruction algorithms (3–6). Alternatively, segmented acquisitions are relatively easy to implement, can be done with standard Fourier reconstruction, and are not as sensitive to field inhomogeneities. Substantial hardware improvements in gradient capabilities on the current generation

Received October 7, 1996; accepted after revision January 16, 1997.
Supported by National Institutes of Health grant RO1HL43812–06.

From the Departments of Diagnostic Radiology (J.A.T., X.D., P.M.R., N.A.O., M.L., T.J.M.) and Biostatistics (N.A.O., M.L.), Cleveland (OH) Clinic Foundation.

Address reprint requests to Jean A. Tkach, PhD, Cleveland Clinic Foundation, Desk L-10, 9500 Euclid Ave, Cleveland, OH 44195.

AJNR 18:1339–1347, Aug 1997 0195-6108/97/1807–1339

of MR imagers now permit relatively short gradient durations, interecho spacing, and absolute echo times to be realized for the segmented gradient-echo studies. Recently, these techniques have been incorporated into three-dimensional time-of-flight (TOF) acquisitions and applied to MR angiography of the intracranial vasculature (R. Gullapalli, M. Loncar, A. Apicella, P. Margosian, "2-D and 3-D Time of Flight Angio Using Interleaved Echo Planar Imaging," in: *Proceedings of the 3rd SMR/12th ESMRMB Joint Meeting,* 1995:584). Alternatively, analogous studies investigating the efficacy of these techniques in imaging the anatomy of the carotid arteries have been comparatively limited (Magnotta et al, "Twenty-three Second..."; J. A. Tkach, X. Ding, P. M. Ruggieri, J. P. Perl, R. Wallace, T. J. Masaryk, "Segmented 3-D EPI for the Evaluation of Cerebrovascular Disease" (poster), in: *Proceedings of the International Society for Magnetic Resonance in Medicine,* 1996:1259; and J. A. Tkach, X. Ding, P. M. Ruggieri, J. P. Perl, R. Wallace, T. J. Masaryk, "Segmented 3-D EPI for the Evaluation of Carotid Disease," presented at the annual meeting of the American Society of Neuroradiology, Seattle, Wash, June 1996).

The purpose of this study was to implement segmented echo-planar 3-D TOF flow sequences, making use of the enhanced gradient capabilities available on current-generation MR imagers, and to apply these techniques to imaging the cervical carotid arteries.

Materials and Methods

The duration of the sampling window, the interecho spacing, and the echo train length (ETL) were systematically manipulated to assess their influence on image quality in healthy volunteers and in patients with known arteriosclerotic disease involving the carotid bifurcation as confirmed by conventional angiography. The various segmented echo-planar 3-D TOF sequences were compared with one another was well as with the conventional (ETL = 1) 3-D TOF technique acquired with similar parameters. The specifics of technique development, image acquisition, and image analysis are described below.

Sequences

The segmented echo-planar imaging and conventional 3-D TOF sequences were implemented and tested on a 1.5-T whole-body MR imager; maximum gradient amplitude was 25 mT/m with a 600-microsecond rise time to maximum amplitude. All images were acquired with the use of a body coil to transmit and a Helmholtz neck coil to receive. With the approval of the internal review board of our institution, imaging examinations were performed in six healthy volunteers (three women and three men, ranging in age from 26 to 54 years) and in five patients (two women and three men, 66 to 79 years of age) with known arteriosclerotic disease involving the carotid bifurcation, as confirmed by conventional angiography. Signed informed consent was obtained from each participant before the start of each examination.

The conventional (ETL = 1) and segmented echo-planar TOF studies were based on a standard radio frequency spoiled sequential 3-D gradient-echo sequence. A tilted nonsaturating excitation pulse (TONE) was used in all sequences. First-order gradient motion refocusing was used in the section-select direction for both the conventional and segmented sequences; the section-select field echo time was 2.168 milliseconds. Acquisition parameters that remained constant among all carotid artery studies were as follows: flip angle of 20°, TONE of 1:2, field of view of 145 mm; in-plane phase encoding was applied right/left, frequency encoding was anteroposterior, three 40-mm axial slabs were collected sequentially against the direction of arterial flow, section distance factor was −0.38, there were 32 section-select partitions; and a superior saturation pulse was applied to eliminate venous flow. For the conventional (ETL = 1) 3-D TOF acquisition, repetition time/echo time (TR/TE) was 48/6.78. The duration of the analog ADC window was 5.12 milliseconds, the echo was collected at 25% asymmetric, and the field echo in the read direction was 4.2 milliseconds. The absolute TE was prolonged to 6.72 milliseconds to achieve a fat/water opposed echo time at 1.5 T to reduce the signal from subcutaneous and intramuscular fat.

In the segmented echo-planar imaging sequences, the in-plane phase-encoding gradient was incremented with each echo within a given echo train. The polarity of the frequency-encoding gradient alternated between successive echoes; the even echoes were time reversed prior to image reconstruction. Centric phase encoding (effective TE = first echo) was used for all of the segmented sequences in an effort to minimize spin dephasing; blipped phase encoding was used to minimize interecho spacing. Phase correction was incorporated into the segmented image reconstruction, and all echoes were acquired symmetrically within the sampling window. Only odd ETLs were implemented such that the associated $T2^*$ filter would be symmetric. Data acquisition times of 2.56, 3.84, and 5.12 milliseconds and ETLs of 3 and 5 were implemented and tested on the healthy volunteers. The aforementioned ADC times corresponded to signal bandwidths of ±50 KHz: 390 Hz/pixel, ±33.3 KHz: 260 Hz/pixel, and ±25 KHz: 195 Hz/pixel, respectively.

First-order gradient motion refocusing was applied for the first echo in each segmented sequence and centric in-plane phase encoding was used. Since the echoes were acquired symmetrically within the data window, the frequency-encoding field echo time for the first echo and associated minimum absolute TEs were somewhat longer for the segmented echo-planar imaging than for those

reported for the conventional (ETL = 1) flow sequence, even for identical signal bandwidths. In addition, odd echoes (echo > 1) benefited from first-order motion compensation in the frequency-encode direction as a result of inherent even echo refocusing of the symmetric gradient waveforms. A representative segmented 3-D echo-planar imaging sequence diagram is provided in Figure 1; the frequency-encode field echo and absolute echo times for the each of the sequences implemented in this study are reported in Table 1. To reduce spatial misregistration of moving tissue, the in-plane phase encoding was placed as close to the start of the sampling window of the first echo (and the only echo for conventional 3-D TOF sequences) as possible. The acquisition parameters were identical to those used for the conventional sequence with the exception of slight differences in TE and the TR, which varied between 34 and 36 for the ETL = 3 segmented echo-planar sequence and between 41 and 58 for the ETL = 5 sequence. The variation in TR and TE (Table 1) reflected the difference in the signal bandwidths and ETLs of the segmented echo-planar imaging sequences. Sagittal-to-coronal maximum intensity projection (MIP) images were generated at 30° increments for each of the MR flow study acquisitions.

Patient examinations were limited to the conventional and two ETL = 3 (data acquisition times of 3.84 [medium bandwidth] and 5.12 [low bandwidth] milliseconds) segmented echo-planar imaging sequences, reflecting the experience gleaned from the volunteer studies. The acquisition parameters for both the conventional and segmented echo-planar imaging studies were identical to those reported previously for the analogous volunteer investigations.

Image Evaluation

The base images of the volunteers produced by each of the segmented and conventional sequences were evaluated quantitatively and qualitatively. The quantitative evaluation was performed assuming the conventional (ETL = 1) MR flow study to be the standard of reference. The dimensions of the common carotid and right vertebral arteries were determined from the original data by measuring the full width half maximum (FWHM) along the in-plane phase-encoding direction (Table 2). To get an accurate measurement of vessel width, the FWHM measurements were made at section locations at which the vessels of interest coursed perpendicular to the through-plane direction. Analogous vessel dimension measurements were also obtained from the associated coronal MIP images at corresponding spatial locations along the section direction (Table 3). In the coronal MIP images, the

TABLE 1: Frequency encode field echo and absolute echo times

ETL/ADC, ms	FE1	TE1	FE2	TE2	FE3	TE3	FE4	TE4	FE5	TE5
a) 1/5.12	4.20	6.72								
b) 3/5.12	7.05	7.82	13.62	14.39	21.04	21.81				
c) 3/3.84	6.38	7.15	11.66	12.43	17.78	18.55				
d) 3/2.56	5.91	6.68	9.91	10.68	14.75	15.52				
e) 5/5.12	6.28	7.82	13.62	14.39	21.04	21.81	28.54	29.31	37.66	38.43
f) 5/3.84	6.38	7.15	11.66	12.43	17.78	18.55	24.74	25.51	32.54	33.31
g) 5/2.56	5.91	6.68	9.91	10.68	14.75	15.52	20.43	21.20	26.95	32.76

Note.—Frequency encode field echo (FE) and absolute echo (TE) times (in milliseconds) for the echo train lengths (ETLs) of 3 and 5 segmented echo-planar and conventional flow sequences implemented in this study. The number of in-plane phase-encoding lines/repeat time, and acquisition time (min:sec) for each of the MR flow examinations are as follows: a) 265/34, 13:55; b) 252/36, 4:50; c) 252/34, 4:34; d) 252/34, 4:34; e) 250/58, 4:44, f) 250/47, 3:50; g) 250/41, 3:20. ADC indicates duration (in milliseconds) of data sampling window.

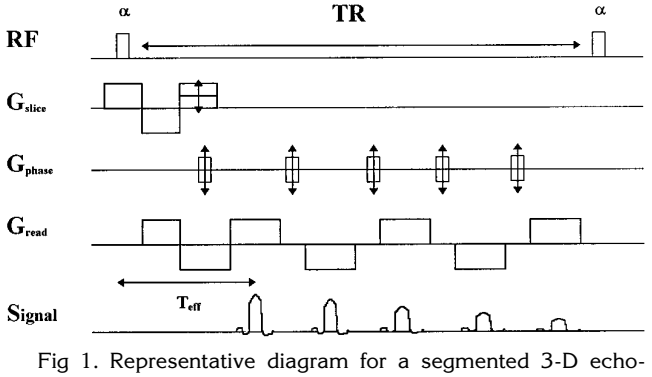

Fig 1. Representative diagram for a segmented 3-D echo-planar flow sequence with ETL of 5 implemented for this study. RF indicates radio frequency; G_{slice}, section select; G_{phase}, in-plane phase encode; and G_{read}, frequency encode. The application of the superior saturation pulse is not included in the diagram.

TABLE 2: Base image vessel normalized FWHM measurements and corresponding sequence ranking

ETL/ADC, ms	Common Carotid Artery		Vertebral Artery	
	FWHM	Sequence Rank	FWHM	Sequence Rank
1/5.12	1.00	1	1.00	1
3/5.12	0.96 ± 0.08	4	0.93 ± 0.26	2
3/3.84	0.93 ± 0.09	2	0.94 ± 0.15	4
3/2.56	0.95 ± 0.05	3	0.97 ± 0.26	3
5/5.12	0.88 ± 0.12	7	0.91 ± 0.15	5
5/3.84	0.93 ± 0.07	6	1.24 ± 0.27	7
5/2.56	0.91 ± 0.06	5	0.87 ± 0.22	6

Note.—In the Results section of the manuscript, the normalized full width half maximum (FWHM) measurement and corresponding sequence ranking are referred to as M3 and M4, respectively. ETL indicates echo train length; ADC, duration of data sampling.

TABLE 3: Maximum intensity projection image vessel normalized FWHM measurements and corresponding sequence ranking

ETL/ADC, ms	Common Carotid Artery		Vertebral Artery	
	FWHM	Sequence Rank	FWHM	Sequence Rank
1/5.12	1.00	1	1.00	1
3/5.12	0.89 ± 0.06	2	0.94 ± 0.11	2
3/3.84	0.91 ± 0.05	3	0.93 ± 0.09	3
3/2.56	0.89 ± 0.09	4	0.97 ± 0.11	4
5/5.12	0.79 ± 0.14	7	0.78 ± 0.17	6
5/3.84	0.78 ± 0.11	6	0.85 ± 0.15	7
5/2.56	0.84 ± 0.07	5	0.82 ± 0.17	5

Note.—In the Results section of the manuscript, these measurements are referred to as M7 and M8, respectively. ETL indicates echo train length; ADC, duration of data sampling window; and FWHM, full width half maximum.

TABLE 4: Base image vessel/muscle normalized contrast measurements and corresponding sequence ranking

ETL/ADC, ms	Common Carotid Artery		Vertebral Artery	
	Contrast with Muscle	Contrast Ranking	Contrast with Muscle	Contrast Ranking
1/5.12	1.00	3	1.00	1
3/5.12	1.06 ± 0.13	1	0.97 ± 0.09	2
3/3.84	1.07 ± 0.16	2	0.94 ± 0.15	3
3/2.56	0.98 ± 0.12	5	0.91 ± 0.04	4
5/5.12	0.94 ± 0.06	6	0.88 ± 0.13	7
5/3.84	0.92 ± 0.08	4	0.87 ± 0.08	6
5/2.56	0.95 ± 0.08	7	0.91 ± 0.06	5

Note.—In the Results section of the manuscript, these measurements are referred to as M1 and M2, respectively. ETL indicates echo train length; ADC, duration of data sampling window.

TABLE 5: Maximum intensity projection image vessel/background normalized contrast measurements and associated sequence ranking

ETL/ADC, ms	Common Carotid Artery		Vertebral Artery	
	Contrast with Background	Contrast Ranking	Contrast with Background	Contrast Ranking
1/5.12	1.00	3	1.00	2
3/5.12	1.10 ± 0.11	1	1.16 ± 0.10	1
3/3.84	1.05 ± 0.08	2	0.99 ± 0.12	3
3/2.56	0.95 ± 0.05	5	0.98 ± 0.03	5
5/5.12	1.00 ± 0.11	4	0.91 ± 0.15	4
5/3.84	0.95 ± 0.10	6	0.92 ± 0.07	6
5/2.56	0.89 ± 0.08	7	0.98 ± 0.08	7

Note.—In the Results section of the manuscript, these measurements are referred to as M5 and M6, respectively. ETL indicates echo train length; ADC, duration of data sampling window.

TABLE 6: MR flow sequence motion rating and corresponding sequence ranking

ETL/ADC, ms	Motion Rating	Sequence Ranking
1/5.12	0.6	4
3/5.12	0.4	3
3/3.84	0.2	2
3/2.56	0.0	1
5/5.12	1.8	7
5/3.84	1.4	6
5/2.56	0.8	5

Note.—The motion rating values reported above were determined by qualitative evaluation of base image data for motion artifacts on a discrete scale of 0 to 3, where 0 = no, 1 = slight, 2 = moderate, and 3 = severe artifacts. ETL indicates echo train length; ADC, duration of data sampling window.

dimension was measured left to right, corresponding to the in-plane phase-encoding direction in the original acquisition. Vessel/muscle and vessel/background contrast measurements were also obtained at analogous locations in both the original and coronal MIP images, respectively, by placing regions of interest in the common carotid and vertebral arteries, muscle, and background.

Prior to final analysis, the contrast and dimensional values were normalized by the analogous measurement in the conventional examination (Tables 4 and 5). The sequences were then ranked on a scale of 1 (best) to 7 (worst) with respect to each of the normalized quantitative measurements. For the dimensional measurements, normalized values not equal to 1 indicated inferior performance. Alternatively, normalized contrast values greater than 1 were considered to indicate superior performance and those less than 1 to indicate inferior performance relative to the conventional examination. For both cases, normalized values equal to 1 inferred equivalent performance.

The relative sensitivity of each of the MR flow studies to motion was determined qualitatively. Corresponding base images acquired with each of the MR flow techniques were evaluated for motion on a scale of 0 to 3, where 0 = no, 1 = slight, 2 = moderate, and 3 = severe artifacts. On the basis of the results of this assessment of the severity of motion artifacts in the base images, the sequences were ranked on a scale of 1 (least severe) to 7 (most severe) (Table 6).

The volunteer MR flow data were also evaluated qualitatively. Specifically, the MIP images generated from each of the MR flow acquisitions (both segmented echo-planar and conventional imaging) for each of the volunteers were ranked by four trained neuroradiologists on a scale of 1 (best) to 7 (worst) (Table 7). The interpreters based their qualitative ranking primarily on signal-to-noise, vessel/background contrast, and artifacts.

The analysis of the patient data was strictly quantitative and performed by two of the four neuroradiologists who evaluated the volunteer data. The segmented echo-planar flow studies were judged for their ability to accurately depict the severity of disease on the MIP images as defined by the percentage of stenosis measured in accordance with criteria developed by the North American Symptom-

TABLE 7: Qualitative sequence ranking

ETL/ADC, ms	Qualitative Sequence Ranking
1/5.12	1.0
3/5.12	2.6
3/3.84	2.85
3/2.56	3.7
5/5.12	6.25
5/3.84	5.8
5/2.56	5.9

Note.—Results of independent qualitative ranking of maximum intensity projection images generated from MR flow examinations in six healthy volunteers. The rating was performed by four trained neuroradiologists on a scale of 1 (best) to 7 (worst) and the results were averaged to produce the reported ranking values. ETL indicates echo train length; ADC, duration of data sampling.

atic Carotid Endarterectomy Trial (NASCET) (7). For this evaluation, the percentage of stenosis measured on the conventional angiogram served as the standard of reference. In anticipation of the potential for flow void to occur at and distal to stenoses that impeded NASCET measurements, such MR angiographic cases were assigned a 99% stenosis value when the distal internal carotid artery was clearly patent.

Statistical Analysis of Quantitative and Qualitative Measurements

Volunteer Data.—The rankings obtained from the quantitative and qualitative measurements were analyzed by means of the Friedman test statistic to determine whether there were any differences in the measurements of the seven MR flow imaging techniques. If the Friedman test was significant at the .05 level, then the following hypotheses were assessed by the Wilcoxon signed rank test: 1) there is no difference in the performance of conventional and segmented echo-planar flow sequences, 2) there is no difference between the performance of ETL = 5 and ETL = 3 segmented echo-planar flow sequences, and 3) there is no difference in the performance of the various-bandwidth ETL = 3 segmented flow sequences. A significance level of .05 was used for all comparisons.

Patient Data.—Independently, for each reader and for each of the MR techniques, using the analysis of variance (ANOVA) procedure, an F test was used to assess the hypothesis that there was no statistically significant difference between the mean percentage of stenosis as obtained by angiography and by each of the MR techniques. Similarly, ANOVA was performed for each reader independently to test the hypothesis that there was no statistically significant difference in performance among the three MR techniques. A significance level of less than .05 was applied.

Results

Volunteer Data

The quantitative vessel dimension analysis performed on the volunteer data indicated that the segmented echo-planar flow studies consistently underestimated the dimension of both large (common carotid) and small (vertebral) arteries on both the original and MIP images (Tables 2 and 3). Exceptions occurred in those studies exhibiting significant (ranking of 2 to 3) motion artifacts caused by swallowing and pulsatile flow. In such instances, vessel dimensions were artifactually increased as compared with the values from the analogous conventional (ETL = 1) examination. Significant motion artifacts were almost exclusively restricted to the ETL = 5 segmented echo-planar studies, increasing in severity with decreasing signal bandwidth. This observation was supported by the qualitatively determined motion rating (Table 6). Another interesting result of the motion analysis was the observation that the ETL = 3 segmented echo-planar sequences exhibited fewer gross motion artifacts than the conventional MR flow examination. This finding probably reflects the increased likelihood of gross patient motion during the relatively long acquisition time required to complete the latter. The uniformity of the signal intensity of the blood was also diminished in the segmented echo-planar images as compared with the conventional study. The nonuniformity was greatest for the ETL = 5 sequences, increasing with decreasing bandwidth. Overall, the subjective impression of the quantitative data was that the ETL = 3 segmented sequences generated superior MR flow images relative to their ETL = 5 counterparts.

As compared with the conventional MR flow images, the ETL = 3 segmented echo-planar sequences exhibited a reduction in vessel dimension (Tables 2 and 3), contrast (Tables 4 and 5), and blood signal uniformity on both the original and MIP images. With respect to signal-to-noise considerations among the various ETL = 3 segmented echo-planar flow techniques, the ±50 KHz sequences were deemed to be inferior to their lower bandwidth counterparts. However, the same data were unable to show a definitive difference or superiority in the performance of the ±33.3-KHz versus the ±25-KHz ETL = 3 segmented sequences.

Statistical analysis of the same quantitative data produced the following results. For five of the quantitative measurements (M3–M5, M7, M8), the performance of the conventional technique was superior to that of the segmented echo-planar flow sequences ($P = .031$), with a

sixth measurement (M6) showing borderline significance ($P = .063$). For seven of the measurements (M1–M5, M7, M8), there was a statistically significant improvement in the performance of ETL = 3 as compared with ETL = 5 segmented echo-planar sequences ($P = .031$), with the eighth measurement (M6) showing borderline significance ($P = .063$). Considering the performance of the ETL = 3 segmented echo-planar sequences, for three (M4–M6) of the quantitative measurements, the low-bandwidth (±25 KHz) sequences were statistically significantly better than their high-bandwidth (±50 KHz) counterparts ($P = .031$).

The qualitative ranking by the radiologists (Table 7) was in agreement with the subjective impression and statistical analysis of the quantitative data. Statistically, all four readers judged the performance of the conventional MR flow technique as superior to that of the segmented echo-planar techniques ($P = .031$). Similarly, for all four readers, there was a statistically significant improvement in the performance of the ETL = 3 as compared with the ETL = 5 segmented echo-planar sequences ($P = .031$). Alternatively, considering the performance of the ETL = 3 segmented techniques alone, there was no statistically significant difference between the low (±25 KHz) and medium (±33.3 KHz) bandwidth sequences. However, for two of the readers, there was a statistically significant improvement in the quality of the medium-bandwidth (±33.3 KHz) segmented echo-planar techniques as compared with that of their high-bandwidth (±50 KHz) counterparts ($P = .031$) and a similar improvement in the performance of the low (±25 KHz) versus high (±50 KHz) bandwidth segmented sequences ($P = .031$).

Patient Studies

As compared with conventional studies, the segmented 3-D echo-planar MR examinations of the patients exhibited a greater nonuniformity in vessel signal. However, artifacts caused by gross patient motion and pulsatile flow were comparable between the ETL = 3 segmented echo-planar and conventional techniques. Except in cases of severe disease (99% stenosis on the angiogram), for which there was complete agreement between the angiographic and MR techniques, the segmented 3-D echo-planar and conventional MR flow techniques consistently overestimated the severity of disease (Fig 2).

For one reader, a comparison of the conventional MR and angiographic techniques showed that the percentage of stenosis seen with conventional MR imaging was, on average, higher than that seen at angiography by 8.2%, which was not statistically significant ($P = .1422$). However, for the second reader, conventional MR imaging showed a higher percentage of stenosis than did angiography by an average of 20.7%, which was significant ($P = .0026$). Comparing the low-bandwidth ETL = 3 segmented 3-D echo-planar (low-bandwidth) technique with angiography, for one reader, the percentage of stenosis seen with the low-bandwidth technique was higher than that seen at angiography by an average of 21.5%, which was significant ($P = .0214$). Similarly, for the second reader, the percentage of stenosis with the low-bandwidth technique was higher than that at angiography by an average of 20.5%, which was also significant ($P = .0496$). Finally, for one reader, the percentage of stenosis seen with the medium-bandwidth segmented MR flow technique was higher than that seen at angiography by an average of 19.1%, which was significant ($P = .0201$). For the second reader, the medium-bandwidth technique showed a higher percentage of stenosis than did angiography by an average of 23.8%, which also was significant ($P = .0046$). In no instance did the segmented 3-D echo-planar imaging or conventional techniques indicate disease that was not present at angiography, resulting in a zero false-positive rate for the MR techniques.

Comparing performance among MR techniques (with respect to angiography), for one reader, there was no statistically significant difference in the performance of the three MR flow techniques ($P = .7964$). For the second reader, however, the conventional MR flow examination provided a marginally statistically significant improvement in performance as compared with the segmented 3-D echo-planar flow techniques ($P = .0583$).

Discussion

The reduction in vessel dimension observed on the segmented echo-planar imaging sequences most likely reflects primarily the effect of the $T2^*$ low-pass filter imposed by the centric reordering scheme used as well as the increase

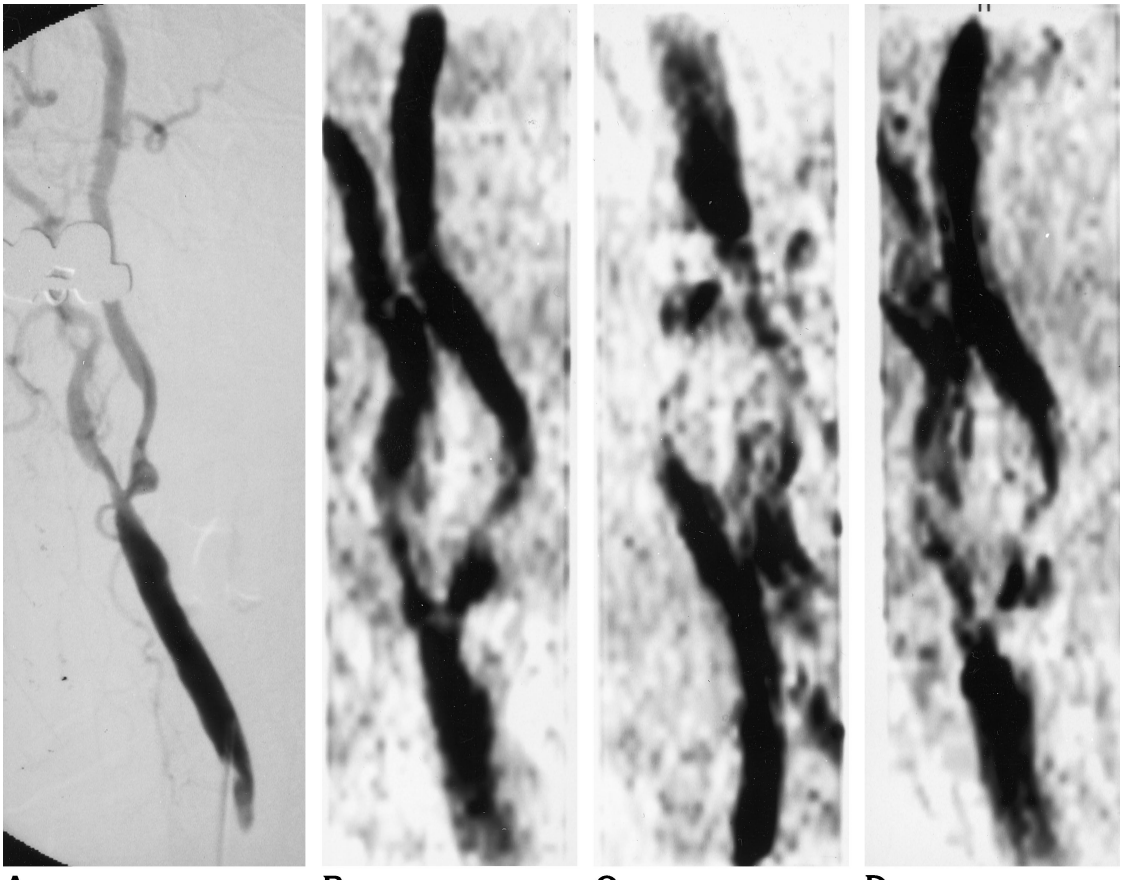

Fig 2. MR flow and angiographic studies acquired in a patient with known carotid occlusion. Angiogram (*A*), conventional MR flow study (*B*), low-bandwidth segmented 3-D echo-planar imaging study (*C*), and medium-bandwidth segmented 3-D echo-planar imaging study (*D*). The TR/TE and matrix size are 34/6.8 and 256 × 256 for the conventional (ETL = 1) acquisition (*B*), 34/7.2 and 252 × 256 for the medium-bandwidth segmented echo-planar imaging acquisition with ETL of 3 (*C*), and 36/7.8 and 252 × 256 for the low-bandwidth ETL = 3 segmented echo-planar imaging acquisition (*D*).

in spin dephasing associated with the longer field echo times (8, 9). As a consequence of its low-pass nature, the reduction in vessel dimension imposed by the filter is greatest for the smaller vessels. The severity of the low-pass filter effect on vessel dimension is dependent on the apparent $T2^*$ of blood. The latter is spatially variant, because it is determined by multiple factors, including the local oxygenation level of the blood ($T2^*$ decreasing with decreasing percentage of O_2), the complexity of flow, and the level of the local static field homogeneity. It is unlikely that the percentage of O_2 in the blood has a large effect on the $T2^*$ value observed in this study. Rather, the local flow patterns (extremely complex at the bifurcation and in regions of stenosis) and static local inhomogeneities (air tissue interface between the chin and neck) were most likely the primary determinants of the local $T2^*$ (10, 11).

The increase in motion artifacts with increasing ETL (3 versus 5) and signal bandwidth is consistent with experience reported with fast spin-echo imaging of the spine as compared with conventional techniques (12). In this study, the increase in motion artifacts with increasing ETL and bandwidth may reflect not only the effect on the larger difference in $T2^*$ decay and accrued transverse spin phase between the different segments of the raw data collected at the different echo times but also to the increased signal from background tissue. The latter is the result of the use of the longer TRs necessitated by the longer ETLs. While the longer TRs allowed for the greater inflow of fresh blood into the imaging volume, it also resulted in an increase in pulsatile motion artifacts in a manner analogous to the increased ghosting observed in large flip angle sequential two-dimensional imaging (13). Nevertheless, the reduction in the

T1 saturation of blood consequent to the increased inflow did not translate into an increase in vessel/background contrast, owing to the proportionately greater increase in signal intensity from the shorter T1 background tissues. Swallowing artifacts were also concomitantly increased. The increase in signal from the background tissues is particularly problematic when the muscle contains a high percentage of fat. The increased sensitivity to motion with the increase in signal intensity from the background tissues indicates that the ETL = 5 sequences are not appropriate for use in patients.

The decrease in blood signal homogeneity in the vessels seen on the original and MIP segmented echo-planar images was due to increased motion artifacts caused by gross patient motion and/or pulsatile flow and increased spin dephasing associated with the longer field echo times. Although the higher signal bandwidth segmented techniques provided shorter field echo times, the sacrifice in signal-to-noise ratio was too severe. The high level of noise degraded the quality of the base images and translated into a loss in vessel information and contrast in the associated MIP images. These observations are consistent with the large body of literature elucidating the importance of and fine line between the influence of signal-to-noise and gradient durations on the quality of MR flow studies (14).

Spatial misregistration of oblique in-plane flow did not seem to be accentuated on the segmented echo-planar sequences. This may in part be attributed to the fact that the in-plane phase-encoding gradient was intentionally applied immediately before the acquisition of the low in-plane spatial frequencies as well as to the fact that the major direction of flow was perpendicular to the through-plane direction. This apparent absence of spatial misregistration of flow will most likely not hold true for applications in which there is significant in-plane flow, such as encountered in flow imaging of the intracranial vasculature (15, 16). Similarly, there was no increase in artifacts caused by the presence of local magnetic field inhomogeneities and/or chemical shift. Nevertheless, this is expected not to be the case when large local magnetic field inhomogeneities are present, suggesting that the performance of the segmented echo-planar imaging techniques would be compromised when applied to flow imaging of the intracranial vasculature (Magnotta et al, "Twenty-three Second..."; Gullapalli et al, "2-D and 3-D...").

The patients' examinations showed that all MR flow techniques overestimated the severity of disease, with the increase greatest for the segmented techniques, independent of signal bandwidth. This finding precludes the use of segmented 3-D echo-planar imaging as a method of obtaining an accurate measurement of the percentage of stenosis upon which subsequent clinical treatment can be determined, as outlined by the results of the NASCET study (7). However, the false-positive rate obtained in this study, together with the substantial reduction in acquisition time, suggests that these techniques may be used for screening/locating studies of cervical carotid disease.

Finally, owing to the large number of statistical comparisons made here, we recognize that the overall type I error rate may exceed the .05 level. However with only six independent cases, our ability to detect real differences would have been near zero if a significance level of less than .05 had been used. We based our conclusions not on any one statistically significant finding but rather on the consistency of the results among the four readers and over the eight quantitative measurements.

Conclusions

Our observations suggest that segmented 3-D echo-planar imaging may fill an important niche in clinical flow imaging of the carotid arteries. Specifically, the segmented 3-D echo-planar sequences can be used as a rapid and accurate screening tool for carotid disease. The inherent $T2^*$ filtering incurred when the ETL was greater than 1 and the increased spin dephasing associated with the longer field echo times preclude the use of segmented echo-planar imaging sequences to obtain accurate estimates of the percentage of stenosis as defined by the NASCET criteria. Nevertheless, the significant reduction in acquisition time provided by these techniques together with the zero false-positive rate obtained suggest that they may be useful as a screening/locating study for carotid disease in certain cases.

References

1. Meyer CH, Hu BS, Nishimura DG, Macovski A. Fast spiral coronary artery imaging. *Magn Reson Med* 1992;28:020–213
2. Yudukevich E, Stark H. Spiral sampling in magnetic resonance

imaging: the effects of inhomogeneities. *IEEE Trans Med Imaging* 1987;MI-6:337–345
3. Farzabeg F, Riederer SJ, Pelc NJ. Analysis of T2 limitations and off-resonance effects on spatial resolution and artifacts in echo-planar imaging. *Magn Reson Med* 1990;14:123–139
4. King KF, Foo TKF, Crawford CR. Optimal gradient waveforms for spiral scanning. *Magn Reson Med* 1995;34:156–160
5. O'Sullivan JD. A fast sinc function gridding algorithm for Fourier inversion in computer tomography. *IEEE Trans Med Imaging* 1985;MI-4:200–207
6. Jackson JI, Meyer CH, Nishimura DG, Macovski A. Selection of a convolution function for Fourier inversion using gridding. *IEEE Trans Med Imaging* 1991;10:473–478
7. North American Symptomatic Carotid Endarterectomy Trial Collaborators. Beneficial effect of carotid endarterectomy in symptomatic patients with high-grade carotid stenosis. *N Engl J Med* 1991;325:445–453
8. Mulkern RV, Wong STS, Winaiski C, Jolesz RA. Contrast manipulation and artifact assessment of 2D and 3-D RARE sequences. *Magn Reson Imaging* 1990;8:556–566
9. Urchuk SN, Plewes DB. Mechanisms of flow-induced signal loss in MR angiography. *J Magn Reson Imaging* 1992;2:453–462
10. Tasciyan TA, Banerjee R, Cho YI, Kim R. Two-dimensional pulsatile hemodynamic analysis in the magnetic resonance angiography interpretation of a stenosed carotid arterial bifurcation. *Med Phys* 1993;20:1059–1070
11. vanTyen R, Saloner D, Jou L-D, et al. MR imaging of flow through tortuous vessels: numerical simulation. *Magn Reson Med* 1994; 31:184
12. Sze G, Kawamura Y, Negishi C, et al. Fast spin-echo MR imaging of the cervical spine: influence of echo train length and echo spacing on image contrast and quality. *AJNR Am J Neuroradiol* 1993;14:1203
13. Tkach JA, Ruggier PM, Ross JR, Modic MT, Masaryk TJ. Pulse sequence strategies for vascular contrast in time-of-flight carotid MR angiography. *J Magn Reson Imaging* 1993;3:811
14. Haacke EM, Masaryk TJ, Wielopolski PA, et al. Optimizing blood vessel contrast in fast-three-dimensional MRI. *Magn Reson Med* 1990;14:202–221
15. Nishimura DG, Jackson JI, Pauly JM. On the nature and reduction of the displacement artifact in flow images. *Magn Reson Med* 1991;22:481–492
16. Frank LR, Buxton RB. Distortions from curved flow in MRI. *J Magn Reson Med* 1993;28:84